Bagua Basin, Peru

Subjects: Geology

Contributor: Federico Moreno , Carmala N. Garzione , Sarah W. M. George , Lauren Williams , Fabiana Richter Oliveira da Silva , Alice Bandeian

Located in northern Peru, at the lowest segment of the Central Andes, the Bagua Basin contains a Campanian to Pleistocene sedimentary record that archives the local paleoenvironmental and tectonic history.

northern Central Andes Bagua Basin

1. Introduction

Nested between the Western and Eastern cordilleras, in the northernmost segment of the Central Andes, the intermontane Bagua Basin contains the sedimentary record of the Late Cretaceous and Cenozoic growth of the Andean mountain belt in this region (**Figure 1**) [1].

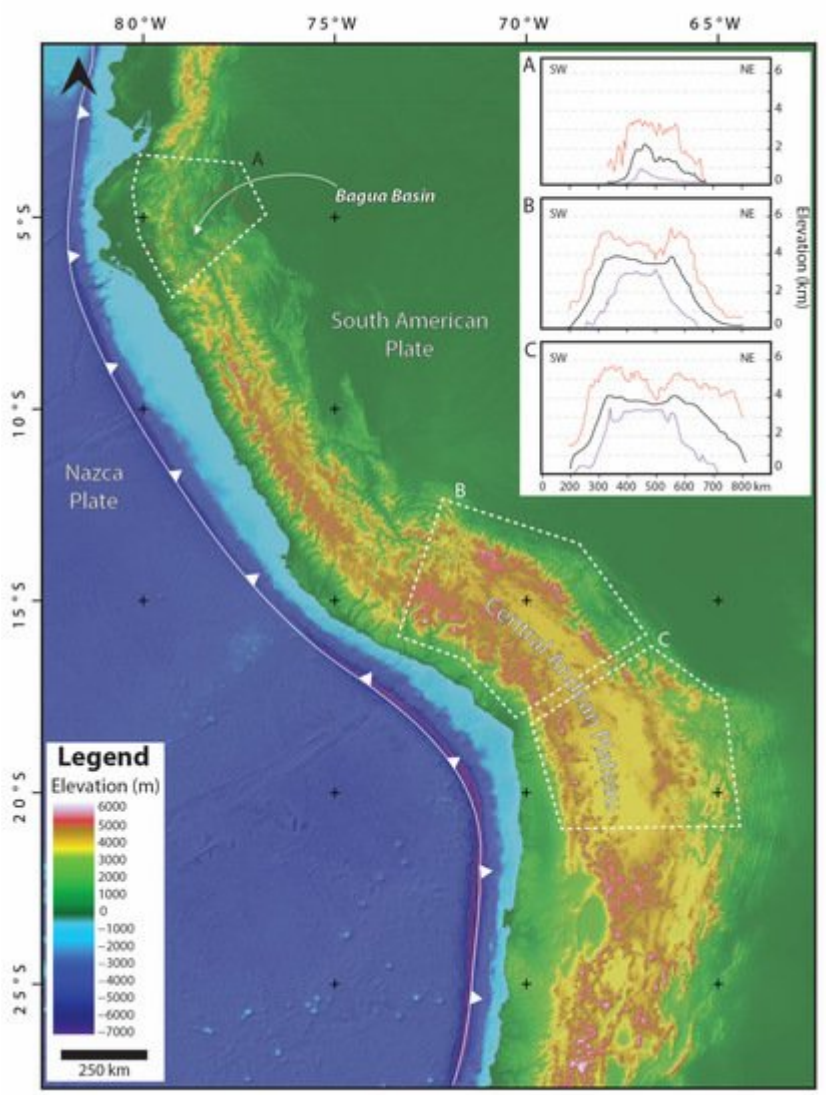

Figure 1. Digital elevation model of the Central Andes showing the location of the Bagua Basin and the Central Andean Plateau. Polygons and swath topographic profiles highlight the contrasting morphology of the (**A**) northernmost Central Andes and (**B**,**C**) the Central Andean Plateau domains. Black line in the swath topographic profiles shows the mean elevation, and orange and purple lines show maximum and minimum elevation, respectively. Swath topographic profiles were constructed using the online tool to produce swath topographic profiles along curved geomorphic features by Hergarten, et al. (2014) [2].

2. Geological Setting

The Central Andes extends from ~3° S to ~33° S along the western margin of the South American plate with a mean elevation of ~2500 m and mean maximum elevation of ~5000 m. The northern termination, between ~3° S and ~7° S, is atypically low with an average elevation of ~1000 m (**Figure 1**). There, the Bagua Basin sits at a mean elevation of 500 m and is flanked by the Eastern and Western cordilleras. At these latitudes the highest peaks of the Western and Eastern cordilleras barely reach 4000 m [3]. The Western Cordillera is composed of the Cretaceous to Cenozoic magmatic arcs, which intruded Paleozoic and Mesozoic metamorphic and sedimentary

rocks that were folded and faulted in the Marañon Fold-Thrust Belt during early Andean orogenesis [4][5]. The Eastern Cordillera is composed of blocks of Paleozoic through Cenozoic rocks uplifted as a result of the inversion of the Permo-Triassic extensional system since the middle Miocene [1][6][7].

In the latest Cretaceous, the tectonic regime in the northernmost Central Andes shifted from dominantly extensional to contractional, resulting in the onset of the Andean orogeny [6]. Three Late Cretaceous–Cenozoic orogenic episodes have been documented in this region [5][8]. An initial pulse of shortening during the latest Cretaceous is characterized by the onset of deformation in the Marañon Fold-Thrust Belt in the Western Cordillera. A second orogenic episode during the Eocene–middle Miocene resulted in the eastward propagation of the deformation front, causing further deformation in the Marañon Fold-Thrust Belt and ultimately capturing the Bagua Basin. A final orogenic episode during the late Miocene–Pliocene was characterized by further migration of the deformation front to the east, causing the inversion of the extensional Permo-Triassic system, resulting in initial deformation of the Eastern Cordillera and subsequent thin skin deformation on the Subandean zone [1][4][5][6][9] (**Figure 2**).

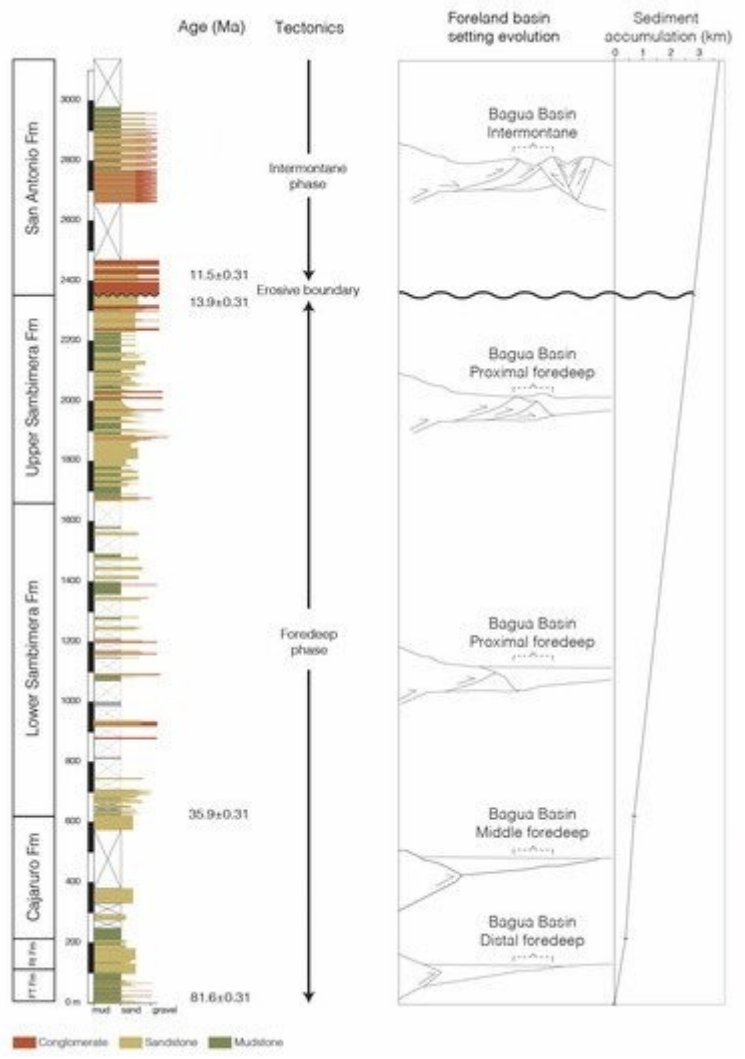

Figure 2. Generalized stratigraphic section of the Campanian to Pliocene sedimentary succession in Bagua Basin. Age constraints are maximum depositional ages from zircon U-Pb geochrononology from Moreno, et al. (2020) [1].

Panels in the left shown from left to right, tectonic and foreland basin setting, and historical de-compacted sediment accumulation curve [1]. Abbreviations: FT Fm = Funfo El Triunfo Formation; Rt Fm = Rentema Formation.

3. Climate and Ecology

The modern climate of the Bagua Basin is hot and dry with marked rainfall seasonality. High and low average temperatures are 32 °C and 20 °C, respectively, while precipitation is ~800 mm/year with most of the rainfall occurring during the wet season October–May [10][11][12]. Tropical dry forest is the prevailing biome in the landscape of the basin [13][14][15]. This precipitation regime and biome composition contrasts with that of the eastern slope of the Eastern Cordillera at the same latitude and altitude (**Figure 3**). There, the climate is characterized by temperatures and rainfall seasonality similar to that of the Bagua Basin, while precipitation is ~3000 mm/year [10][11][12], and the biome composition is dominated by tropical moist forest [13][14][15]. These contrasting climatic and ecological conditions are the result of the rain-shadow effect exerted by the Eastern Cordillera that serves as a barrier for the low-level warm and moist trade winds travelling from the east, thereby causing its adiabatic cooling and subsequent precipitation on the eastern slope of the orogen [10][16][17]. The moisture that precipitates in this region originates in the Atlantic Ocean, is transported to the west by the trade winds that converge in the Intertropical Convergence Zone [18], and it is largely affected by the evapotranspiration of vegetation during its ~4000 km traverse over the Amazon forest [19].

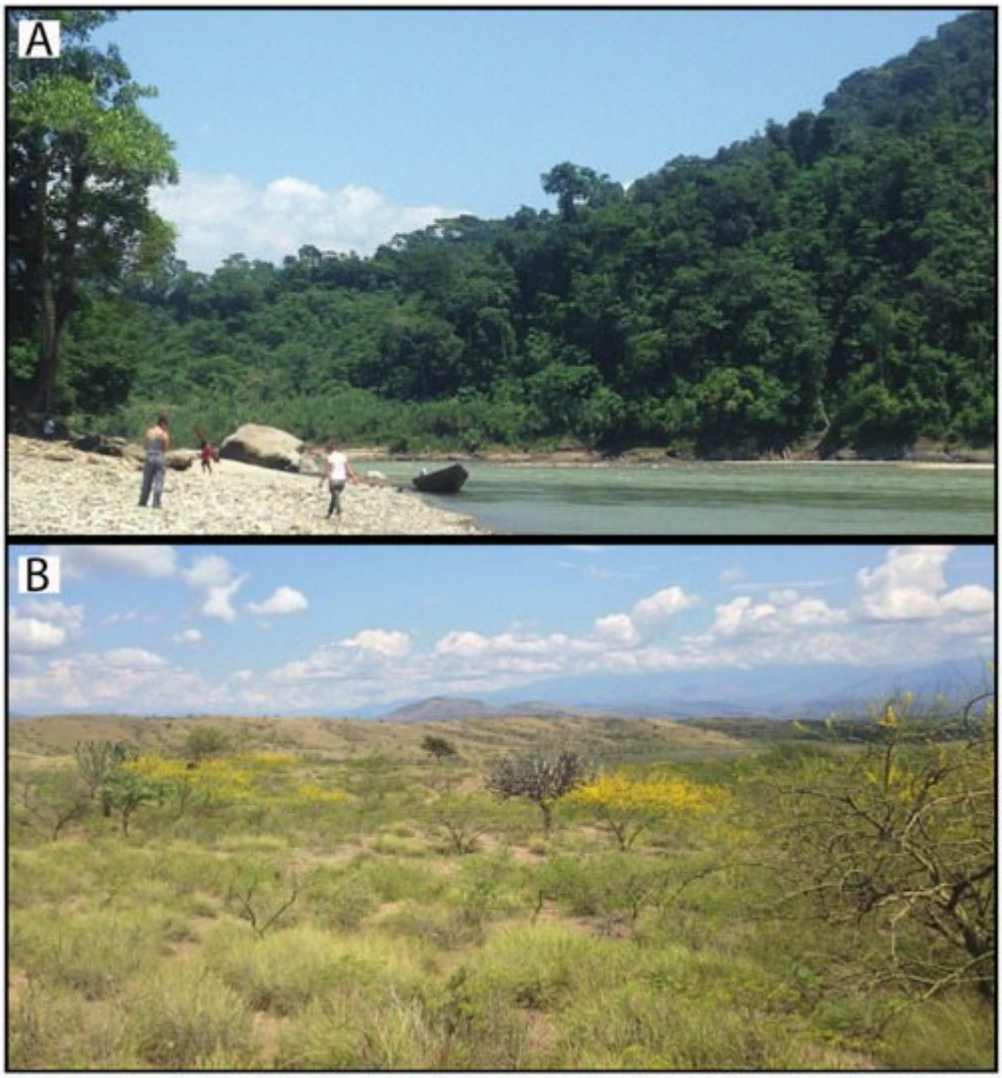

Figure 3. Photographs showing the contrasting landscape between (**A**) the eastern slope of the Eastern Cordillera and the (**B**) Bagua Basin at the same latitude.

4. Basin Evolution and Stratigraphy

The Bagua Basin contains a protracted sedimentary record of the Late Cretaceous and Cenozoic tectonic history of the northernmost Central Andes [1]. Onset of shortening in the latest Cretaceous resulted in the development of a foreland basin as a response to the tectonic load of the nascent orogen. Deposits related to this shortening event are chronicled in the middle Campanian–Maastrichtian Fundo El Triunfo Formation, which contains the distal foredeep sedimentary deposits of a meandering fluvial system. Sedimentation in the distal foredeep continued during the Paleocene–earliest Eocene with the braided fluvial deposits of the Rentema Formation. During the Eocene–middle Miocene, the deformation front advanced eastward, causing a progressive increase in subsidence rates in the Bagua Basin. The Eocene Cajaruro Formation was deposited in a fluvio-lacustrine system in a middle foredeep setting, and the upper Eocene–Oligocene lower Sambimera Formation represents a meandering fluvial system in a proximal foredeep setting. The deformation front continued to migrate to the east, capturing the Bagua

Basin in the middle Miocene. At that time, the upper Sambimera Formation was deposited in a wedge top setting. An erosive boundary separates the Sambimera Formation from the San Antonio Formation. This boundary records the final transit of the deformation front eastward of the basin. The upper Miocene–Pliocene San Antonio Formation contains the deposits of a fluvio-lacustrine system active in an intermontane setting that resulted from the initial uplift of the Eastern Cordillera. The Pleistocene conglomerates of the Tamborapa Formation and Holocene sandy and gravely deposits, cap the sedimentary succession. Details of the Campanian–Pliocene evolution of the foreland Bagua Basin are discussed in Moreno, et al. (2020) [1].

Paleosols in the Bagua Basin

Paleosols occur in the middle Campanian–Maastrichtian Fundo El Triunfo Formation and in the upper Eocene–middle Miocene Sambimera Formation. In the Fundo El Triunfo Formation, paleosols occur in the upper part of the up-to-20-m-thick bodies of stacked mudstone beds that represent flood plain deposits. The paleosols are red, massive, fine grained, and contain root traces in their upper part. Toward the base their color fades to mottled purple-grey, and the grain size is coarser. Pedogenic carbonate nodules are incipient, reaching a few millimeters in size, and occurring at ~70–100 cm from the top of the paleosol (**Figure 4**).

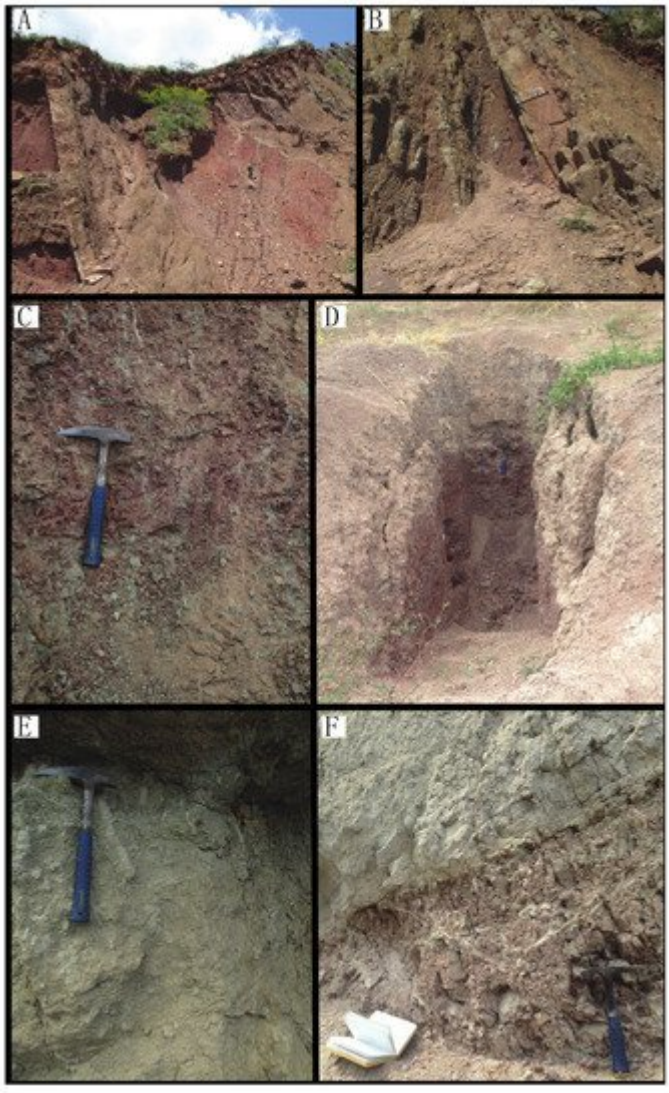

Figure 4. Paleosols photographs from the Fundo El Triunfo Formation (**A**,**B**) and the Sambimera Formation (**C**–**F**).

Paleosols in the Sambimera Formation occur throughout the thickness of the unit (~1600 m) in floodplain intervals. Paleosols show strong color and texture change across the pedogenic profile from red, clay-sized and massive at the top, fading to light red to light grey mottled in the middle part, and to light grey with coarser grain (silt to sand) and crude laminations at the base. They preserve root traces in the upper part, and pedogenic carbonate nodules toward the middle part between ~70 cm and 1.5 m from the top. The size of carbonate nodules varies from millimeters up to a few centimeters for well-developed nodules (**Figure 4**).

References

1. Moreno, F.; Garzione, C.N.; George, S.W.M.; Horton, B.K.; Williams, L.; Jackson, L.J.; Carlotto, V.; Richter, F.; Bandeian, A. Coupled Andean Growth and Foreland Basin Evolution, Campanian–Cenozoic Bagua Basin, Northern Peru. Tectonics 2020, 39, e2019TC005967.
2. Hergarten, S.; Robl, J.; Stüwe, K. Extracting topographic swath profiles across curved geomorphic features. Earth Surf. Dyn. 2014, 2, 97–104.
3. Montgomery, D.R.; Balco, G.; Willett, S.D. Climate, tectonics, and the morphology of the Andes. Geology 2001, 29, 579–582.
4. Scherrenberg, A.F.; Kohn, B.P.; Holcombe, R.J.; Rosenbaum, G. Thermotectonic history of the Marañón Fold–Thrust Belt, Peru: Insights into mineralisation in an evolving orogen. Tectonophysics 2016, 667, 16–36.
5. Mégard, F. The Andean orogenic period and its major structures in central and northern Peru. J. Geol. Soc. 1984, 141, 893–900.
6. George, S.W.; Horton, B.K.; Jackson, L.J.; Moreno, F.; Carlotto, V.; Garzione, C.N. Sediment provenance variations during contrasting Mesozoic-early Cenozoic tectonic regimes of the northern Peruvian Andes and Santiago-Marañón foreland basin. In Andean Tectonics; Horton, B.K., Folguera, A., Eds.; Elsevier: Amsterdam, The Netherlands, 2019; pp. 269–296.
7. Pfiffner, A.; Gonzalez, L. Mesozoic–Cenozoic Evolution of the Western Margin of South America: Case Study of the Peruvian Andes. Geosciences 2013, 3, 262–310.
8. Noble, D.C.; McKee, E.H.; Mourier, T.; Mégard, F. Cenozoic stratigraphy, magmatic activity, compressive deformation, and uplift in northern Peru. Geol. Soc. Am. Bull. 1990, 102, 1105–1113.
9. Eude, A.; Roddaz, M.; Brichau, S.; Brusset, S.; Calderon, Y.; Baby, P.; Soula, J.-C. Controls on timing of exhumation and deformation in the northern Peruvian eastern Andean wedge as inferred from low-temperature thermochronology and balanced cross section. Tectonics 2015, 34, 715–730.

10. Bookhagen, B.; Strecker, M.R. Orographic barriers, high-resolution TRMM rainfall, and relief variations along the eastern Andes. Geophys. Res. Lett. 2008, 35.
11. Weather Spark. Available online: https://weatherspark.com/ (accessed on 13 April 2022).
12. Climate Data Climate Data for Cities Worldwide—Climate-Data.Org. Available online: https://en.climate-data.org/ (accessed on 13 April 2022).
13. Särkinen, T.; Iganci, J.R.; Linares-Palomino, R.; Simon, M.F.; E Prado, D. Forgotten forests—Issues and prospects in biome mapping using Seasonally Dry Tropical Forests as a case study. BMC Ecol. 2011, 11, 27.
14. Olson, D.M.; Dinerstein, E.; Wikramanayake, E.D.; Burgess, N.D.; Powell, G.V.N.; Underwood, E.C.; D'Amico, J.A.; Itoua, I.; Strand, H.E.; Morrison, J.C.; et al. Terrestrial Ecoregions of the World: A New Map of Life on Earth: A New Global Map of Terrestrial Ecoregions Provides an Innovative Tool for Conserving Biodiversity. Bioscience 2001, 51, 933–938.
15. Eva, H.D.; Belward, A.S.; De Miranda, E.E.; Di Bella, C.M.; Gond, V.; Huber, O.; Jones, S.; Sgrenzaroli, M.; Fritz, S. A land cover map of South America. Glob. Chang. Biol. 2004, 10, 731–744.
16. Garreaud, R.D. The Andes climate and weather. Adv. Geosci. 2009, 22, 3–11.
17. Garreaud, R.; Vuille, M.; Compagnucci, R.; Marengo, J. Present-day South American climate. Palaeogeogr. Palaeoclim. Palaeoecol. 2009, 281, 180–195.
18. Bershaw, J.; Saylor, J.; Garzione, C.N.; Leier, A.; Sundell, K.E. Stable isotope variations (δ18O and δD) in modern waters across the Andean Plateau. Geochim. Cosmochim. Acta 2016, 194, 310–324.
19. Vuille, M.; Bradley, R.S.; Werner, M.; Healy, R.; Keimig, F. Modeling δ 18 O in precipitation over the tropical Americas: 1. Interannual variability and climatic controls. J. Geophys. Res. Earth Surf. 2003, 108, D6.